Stem Cell Research & Therapy

RESEARCH

Open Access

Circ-AARS plays an important role during the odontogenic differentiation of dental pulp stem cells by modulating miR-24-3p/KLF6 expression

Meizhi Sui[1,3†], Jiaxuan Lyu[1†], Jiaxin Zhou[1], Qian Liao[1,3], Zexu Xiao[2], Mingming Jin[2*] and Jiang Tao[1*]

Abstract

Background Circular RNAs (circRNAs) play a crucial role in stem cell-based tooth regeneration. However, the functions and underlying mechanisms of circRNAs in tooth regeneration from human dental pulp stem cells (DPSCs) remain largely unclear.

Methods In this study, DPSCs were used for odontogenic differentiation. High-throughput sequencing was performed for differential circRNA analysis. A luciferase reporter assay was conducted to confirm the downstream target of the circRNA, circ-AARS. We then constructed vectors and siRNAs for overexpressing and silencing circ-AARS, miR-24-3p, and Krüppel-like factor 6 (KLF6) and transfected them into DPSCs. Alkaline phosphatase staining, Alizarin Red S staining, western blotting assay, and quantitative reverse transcription-polymerase chain reaction were used to explore the underlying mechanisms of circ-AARS. Finally, a heterotopic bone model was utilized to reveal the regulating effects of circ-AARS.

Results High-throughput sequencing analysis showed that circ-AARS plays an important role during the odontogenic differentiation of DPSCs. Downregulation of circ-AARS inhibited the odontogenic differentiation of DPSCs; however, circ-AARS overexpression promoted their odontogenic differentiation. Bioinformatics analysis and luciferase reporter assay confirmed that both miR-24-3p and KLF6 were the downstream targets of circ-AARS. miR-24-3p downregulation or KLF6 overexpression restored the odontogenic differentiation ability of DPSCs after circ-AARS silencing. KLF6 upregulation restored the odontogenic differentiation ability of DPSCs after KLF6 overexpression. The heterotopic bone model confirmed that circ-AARS overexpression promoted the odontoblastic differentiation of DPSCs.

Conclusion The present study showed that circ-AARS can promote the odontoblastic differentiation of DPSCs by increasing KLF6 expression and sponging miR-24-3p. Taken together, the results indicate that circ-AARS may be a potential positive regulator of odontoblastic differentiation of DPSCs.

Keywords Circ-AARS, Odontogenic differentiation, Dental pulp stem cells

†Meizhi Sui and Jiaxuan Lyu have contributed equally to this work and share first authorship.

*Correspondence:
Mingming Jin
asdjinmingming@126.com
Jiang Tao
taojiang_doctor@sjtu.edu.cn
Full list of author information is available at the end of the article

Background

Dental pulp tissue regeneration can serve as a clinically relevant treatment to replace the existing root canal therapy used for treating necrotic permanent teeth [1]. Dental pulp stem cells (DPSCs) are a type of mesenchymal stem cells with self-renewal and multilineage differentiation capabilities [2]. Previous studies have confirmed that DPSCs can be used as biomimetic tools to induce odontogenic differentiation of stem cells during dental pulp regeneration [3]. However, the mechanisms that promote dentin differentiation of DPSCs remain unclear.

Circular RNAs (circRNAs) are a type of endogenous molecules without 5′-cap and 3′-poly (A) tail [4]. Because of their round structure, circRNAs cannot be degraded by exonucleases and show higher stability than other linear RNAs [5]. CircRNAs harbor microRNA (miRNA) binding sites, which normally function as miRNA sponges [6, 7]. Previous studies have confirmed that circ_0005564 is a potential positive regulator of osteogenic differentiation of bone marrow stromal cells [7]. Hsa_circ_0026827 promotes osteoblast differentiation of DPSCs through Beclin1 and RUNX1 signaling pathways by sponging miR-188-3p, which could act as a novel therapeutic strategy for treating osteoporosis [8]. In this study, circRNA expression profile analysis revealed that circ-AARS is abnormally expressed during the odontogenic differentiation of DPSCs; however, its function remains unclear. Therefore, the present study evaluated the role of circ-AARS in the odontogenic differentiation of DPSCs. The findings suggest candidate therapeutic strategies for dentin regeneration and reveal novel mechanisms underlying osteogenic differentiation.

Materials and methods

Ethics statement

This animal-based study was reported according to Preferred Reporting Items for Animal Studies in Endodontology 2021 guidelines [9]. This study was reviewed and approved by the Ethics Committee of the Shanghai Ninth People's Hospital, Shanghai Jiao Tong University School of Medicine (SH9H-2021-A939-1).

Isolation, culturing, and differentiation of human DPSCs (hDPSCs)

After receiving approval from the institutional ethics committee and informed consent from the participants, hDPSCs were isolated from the orthodontically extracted teeth of eight subjects aged 10–12 years. The extracted teeth were transported on ice, and their dental pulp was extracted, minced, and incubated with type I collagenase within 4 h of extraction. This processed tissue was cultured in T25 flasks containing α-MEM (HyClone) supplemented with 10% fetal bovine serum (FBS; Bioexplorer) and 1% penicillin/streptomycin (Gibco) at 37 °C in a 5% CO_2 atmosphere. After achieving cell confluence of 70–80%, the cells were passaged into new flasks. Cells from the third to fifth passages at 70–80% confluence were subsequently cultured in an osteogenic differentiation medium (OriCell) for further experimental studies. This study was reviewed and approved by the Ethics Committee of the Shanghai Ninth People's Hospital, Shanghai Jiao Tong University School of Medicine (No. SH9H-2021-T425-1), and written informed consent forms were obtained from all patients.

Flow cytometry analysis

Cells from the third passage of DPSCs were enzymatically dissociated, centrifuged, and counted. Subsequently, 1×10^6 cells were resuspended in phosphate-buffered saline (PBS). Fluorescein isothiocyanate-conjugated antibodies, used at 1:100 dilution according to the manufacturer's recommendation, were added to the cells. The following antibodies (Biolegend) were used along with corresponding isotype control antibodies: anti-CD45, anti-CD90, anti-CD105, anti-CD73, and anti-CD31. The cells were incubated in darkness for 30 min. Subsequently, the cells were washed with PBS containing 2% FBS. Cell surface antigen detection was then performed with a flow cytometer (NovoCyte 2, Agilent, USA), which facilitated the immunophenotypic analysis of the cells.

Bioinformatics analysis

By using RNA sequencing and integrating the data from various databases such as circBank, starBase, TargetScan, and miRDB, we predicted target miRNAs for hsa_circ_0040158 and their corresponding target genes. These predicted target genes were then compared with the genes showing differential expression, which enabled to identify differentially expressed target genes. This methodology played an instrumental role in constructing the regulatory network associated with hsa_circ_0040158.

Plasmid construction and transfection

Lentiviruses were engineered by GenePharma Co., Ltd. (Shanghai, China). After achieving 50% cell confluence, these lentiviruses were used to infect hDPSCs to mediate both inhibition and overexpression of hsa_circ_0040158. A Krüppel-like factor 6 (KLF6)-overexpressing plasmid, synthesized by GenePharma Co., Ltd., was introduced into hDPSCs by using the same approach. Lipofectamine 2000 (Invitrogen Life Technologies, USA) was utilized for transfecting the miR-24-3p mimics, miR-24-3p inhibitors, and corresponding negative controls. The cells were then collected, and transfection success was assessed by quantitative reverse transcription-polymerase chain reaction (qRT-PCR).

Dual-luciferase reporter (DLR) assay

For luciferase activity assays, wild-type and miR-24 binding site-deleted hsa_circ_0040158 clones were co-transfected into cells along with a plasmid expressing the miR-24 precursor. Clones of the KLF6 3′-UTR and its miRNA binding site deletion mutants were also prepared and co-transfected with miRNA-overexpressing vectors into cells to measure both Renilla and firefly luciferase activities.

qRT-PCR

Following washing with 1×PBS, total RNA was carefully extracted from cells by using an RNA extraction kit (Vazyme, China). The purity and concentration of the RNA samples were accurately determined using a spectrophotometer (Thermo Fisher, USA). Reverse transcription of circRNA and miRNA was achieved using the PrimeScript RT Reagent Kit (Takara Bio, Japan) and the miRNA 1st Strand cDNA Synthesis Kit (Vazyme), respectively. To quantify cDNA, SYBR Green PCR Master Mix (Vazyme) was used in the QuantStudio 7 Flex Real-Time PCR System (Applied Biosystems, USA). Threshold cycle (Ct) values were established, and the relative expression levels of the target genes were calculated using the $2^{-\Delta\Delta Ct}$ method, with normalization against GAPDH and U6 expression levels. Table 1 shows the primers for all target genes investigated in this study.

Western blotting (WB) assay

Cells were lysed using RIPA lysis buffer (Beyotime, Shanghai, China), and the protein content was quantified using the BCA Protein Assay Kit (Beyotime). Proteins were separated by electrophoresis, and the separated proteins were transferred onto polyvinylidene fluoride membranes. The membranes were blocked with 5% non-fat milk at room temperature for 1 h and then incubated overnight at 4 °C under gentle agitation with primary antibodies against ALP (Abways, 1:2000), RUNX2 (ABclonal, 1:500), OPN (ABclonal, 1:1000), OCN (ABclonal, 1:1000), DMP1 (SAB, 1:500), DSPP (Affinity, 1:500), and GAPDH (Proteintech, 1:50,000). On the next day, the membranes were washed three times with Tris-buffered saline containing 0.1% Tween-20, followed by 1 h incubation with HRP-conjugated anti-rabbit/mouse IgG secondary antibodies (Proteintech, 1:10,000). After three additional washes, protein bands on the X-ray film were visualized using a chemiluminescence imaging system (Tanon 5200 Multi Chemiluminescence Imaging System, Tanon Science & Technology, China). Protein expression levels were normalized to that of GAPDH, and the ratio of target protein levels was calculated.

Alkaline phosphatase (ALP) staining

ALP expression was detected using the NBT/BCIP staining kit (Beyotime). The culture medium was discarded, and cells were washed with PBS. The cells were then fixed at room temperature with 4% paraformaldehyde (PFA; Beyotime) and subsequently washed with PBS (HyClone). The ALP staining solution was applied to the cells, and the cells were incubated in the dark for 30 min. After removing the ALP staining solution, the cells were washed with PBS. The stained cells were observed under an inverted phase contrast microscope (DMi1; Leica, China).

Determination of ALP activity

Following washing with PBS, the cells were subjected to a 30-min lysis process by using 1% Triton X-100 (Beyotime). Subsequently, the supernatant was carefully

Table 1 Primers for real-time polymerase chain reaction (RT-qPCR) in this study

Gene markers	Primer sequences	
	Forward	Reverse
hsa_circ_0040158	CCCCGCATTGCTGTTGAT	CGCACGTGGTCCTTTTATTC
KLF6	GACAGCTCCGAGGAACTTTCT	CACGCAACCCCACAGTTGA
DSPP	CAACCATAGAGAAAGCAAACGCG	TTTCTGTTGCCACTGCTGGGAC
RUNX2	TGGTTACTGTCATGGCGGGTA	TCTCAGATCGTTGAACCTTGCTA
ALP	ACTGGTACTCAGACAACGAGAT	ACGTCAATGTCCCTGATGTTATG
OPN	GGAGTTGAATGGTGCATACAAGG	CCACGGCTGTCCCAATCAG
DMP1	CTCCGAGTTGGACGATGAGG	TCATGCCTGCACTGTTCATTC
OCN	AGCCACCGAGACACCATGAGA	GGCTGCACCTTTGCTGGACT
miR-24-3p	GGCTGCACCTTTGCTGGACT	–
GAPDH	GGAGCGAGATCCCTCCAAAAT	GGCTGTTGTCATACTTCTCATGG

collected to assess both the protein concentration and ALP activity by using the ALP Activity Assay Kit (Nanjing Jiancheng Bioengineering Institute, China). The optical density (OD) of each sample was carefully measured at 520 nm wavelength. Based on these measurements, the relative ALP activity for each sample was accurately calculated.

Alizarin red S (ARS) staining

To detect calcium nodule deposition on DPSCs during the advanced phase of osteogenic induction, the cells at 21 days post-induction were washed twice with PBS and then fixed at room temperature with 4% PFA. After a subsequent washing step with PBS, the cells were stained in the dark for 30 min by using an ARS solution (OriCell, China). The staining solution was removed, and the stained cells were washed with PBS and carefully examined under an inverted phase contrast microscope (DMi1; Leica) for detailed observation.

ARS quantification

To extract mineralized deposits, the ARS dye was washed off with 10% cetylpyridinium chloride. The OD of each sample was measured at 562 nm wavelength to evaluate the degree of calcification. Concurrently, the protein concentration was determined for relative ARS semi-quantification in each sample.

Heterotopic implantation of hDPSCs for bone formation assay

hDPSCs (NC) and hDPSCs transfected with lentivirus silence negative control (sh-NC), lentivirus circ_0040158 silence (sh-circ_0040158 and sh-circ-AARS), lentivirus overexpression negative control (LV-NC), and circ_0040158 overexpression (lv-circ_0040158 and lv-circ-AARS) underwent osteogenic induction for 7 days. Post-induction, the cells were digested, centrifuged, and seeded onto silk fibroin sponge scaffolds. These scaffolds were randomly implanted into the dorsal region of 10 BALB/c nude mice, with each mouse receiving one implant on the either side. The incisions were then sutured. The mice were placed in a quiet environment for 5–10 min to acclimatize to reduce the stress response. Subsequently, the mice were placed in the anesthesia box, the gas flow control system was started, the oxygen flow was set to 1–2 L/min, and the isoflurane concentration was adjusted to 4–5%. Within 1–2 min, the mice could be seen to slow down breathing, reduce or stop movement, and enter the anesthesia state. When the mice have no spontaneous motor or reflex response, the anesthetic concentration can be reduced to 1–2% to maintain anesthesia. The physiological state of the mice was monitored during anesthesia, that is, the respiratory rate was in the normal range of 60–100 times/minute; The normal range of heart rate is 400–600 beats/min. An electric blanket was used to maintain the mice's body temperature. External stimulation ensured that the mice were completely anesthetized for subsequent experimental operations. After the experiment was completed, the isoflurane concentration was gradually reduced to 0% and only oxygen flow was maintained to help the mice clear the anesthetic gas from their bodies. After about 5–10 min, the mice gradually regain consciousness and begin to show spontaneous activity. Finally, it was placed in the cage alone to observe its recovery.After 8 weeks, The mice were humanely euthanized using 100% carbon dioxide, and the implants were retrieved for further examination.

Hematoxylin–eosin (H&E) staining, masson's trichrome staining, and immunohistochemistry (IHC)

Post-implant fixation, the specimens were subjected to a 7-day dehydration process and paraffin-embedded for sectioning. These sections were stained with H&E and Masson's trichrome stain. The sections were incubated with primary antibodies against BGLAP (Santa Cruz, USA) at overnight at 4 °C, followed by washing with PBS. The sections were then treated with HRP-conjugated goat anti-rabbit IgG secondary antibodies (dilution 1:200), Finally, the cell nuclei were stained with DAPI, and images of the stained cells were acquired for further examination.

Statistical analysis

Statistical analysis was performed using Prism 8.0 software (GraphPad, CA, USA). For pairwise comparison, the least significant difference t-test method was used. For comparison of multiple groups, one-way ANOVA was used for normally distributed data, and the Friedman test was used for non-normally distributed data. A p-value of < 0.05 denoted statistical significance.

Results

Circ-AARS plays a role during the odontogenic differentiation of DPSCs

Here, we successfully isolated DPSCs from pulp tissue. The isolated DPSCs showed a typical shuttle-shaped morphology (Fig. 1A). Flow cytometry analysis of DPSCs revealed negative expression of CD34, CD45 (< 20%), and HLA-DR, together with positive expression of CD90, CD105, and CD73 (> 90%) (Fig. 1B–H). This finding confirmed that the isolated cells were DPSCs.

We found that DPSCs exhibited osteogenic differentiation ability based on the results of ALP staining (Fig. 2A and B) and ARS staining (Fig. 2C and D). Western blot assay results showed that the expression levels of ALP, OPN, DSPP, OCN, DMP1, and RUNX2 were increased

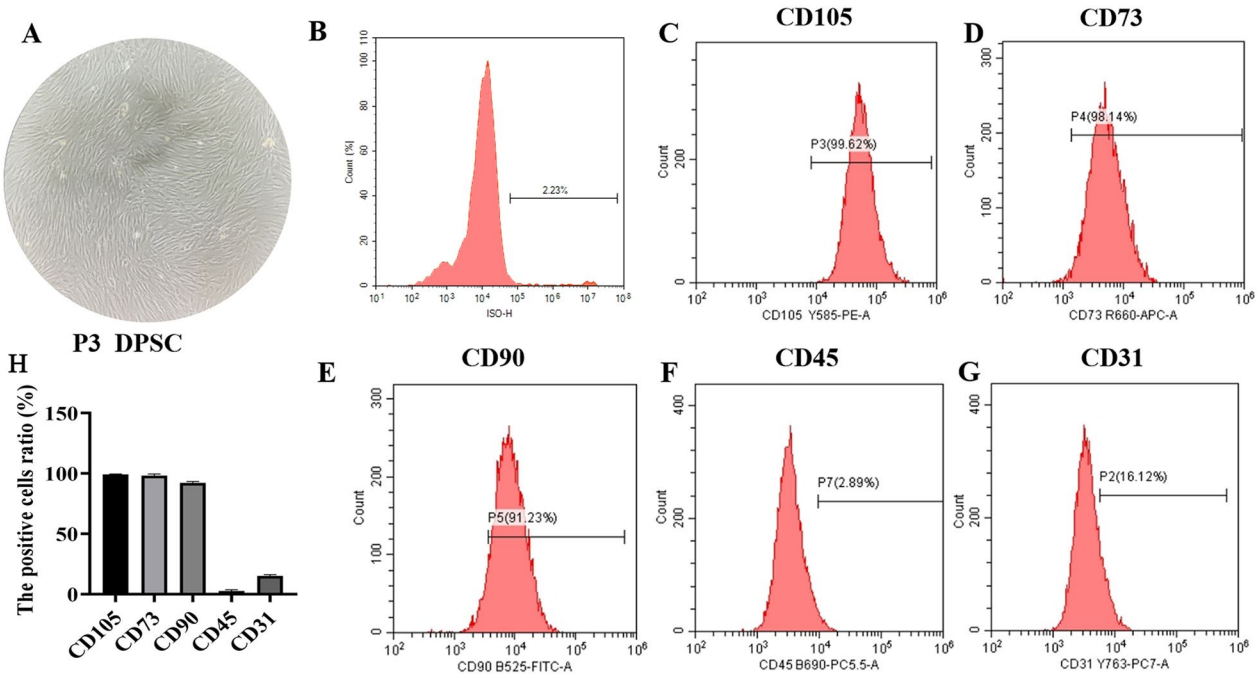

Fig. 1 Characterization of dental pulp stem cells (DPSCs). **A** DPSCs show a typical shuttle-shaped morphology. **B**–**G** Flow cytometry analysis of DPSCs revealed negative expression of CD34, CD45, and HLA-DR and positive expression of CD90, CD105, and CD73. H The positive cell ratio of DPSCs for different protein markers

during the odontogenic differentiation of DPSCs (Fig. 2E and F). To identify circRNAs with a differential expression pattern, normal DPSCs and those in the stage of odontogenic differentiation were analyzed by high-throughput sequencing. The results showed a large number of differentially expressed circRNAs (Fig. 2G). qRT-PCR analysis revealed that hsa_circ_0040158 expression was increased significantly in DPSCs during their odontogenic differentiation (Fig. 2H). qRT-PCR also confirmed that the relative gene expression levels of ALP, OPN, DSPP, OCN, DMP1, and RUNX2 were increased in DPSCs during odontogenic differentiation (Figs. 2I–O).

Circ-AARS plays an important role in promoting the odontogenic differentiation of DPSCs

According to our bioinformatics analysis (http://www.circbase.org/), hsa_circ_0040158 originates from the exon of the AARS gene located at chr16:70,286,296–70287284. The AARS gene is 899 bp in length, and the spliced mature circRNA is 627 bp in length; hence, we designated hsa_circ_0040158 as circ-AARS (Fig. 3A). Fluorescence in situ hybridization showed that circ-AARS is mainly localized in the cytoplasm (Fig. 3B). Circ-AARS was constructed with 2 exons of the AARS gene (Fig. 3C). Sanger sequencing confirmed the sequences amplified by divergent primers (Fig. 3D). The amplification products obtained with divergent primers and convergent primers were separated by agarose gel electrophoresis (Fig. 3E). These findings confirmed that circ-AARS was circRNA and originated from the AARS gene.

ALP staining (Fig. 4A and B) and ARS staining (Fig. 4C and D) showed that the odontogenic differentiation of DPSCs was inhibited after circ-AARS downregulation. qRT-PCR analysis showed that circ-AARS expression was decreased after transfection with the circ-AARS silencing vector (Fig. 4E). qRT-PCR analysis also showed that the mRNA expression levels of ALP, OPN, DSPP, OCN, DMP1, and RUNX2 were decreased during the odontogenic differentiation of DPSCs after circ-AARS downregulation (Fig. 4F–K). WB assay results showed that the protein expression levels of ALP, OPN, DSPP, OCN, DMP1, and RUNX2 were decreased during the odontogenic differentiation of DPSCs following circ-AARS downregulation (Fig. 4L and M). These findings suggest that circ-AARS downregulation inhibits the odontogenic differentiation of DPSCs.

qRT-PCR analysis demonstrated that circ-AARS expression increased following transfection with the circ-AARS-overexpressing vector (Fig. 5A). ALP staining (Fig. 5B and C) and ARS staining (Fig. 5D and E) showed increased odontogenic differentiation ability of DPSCs after circ-AARS upregulation. qRT-PCR analysis revealed that the mRNA expression levels of ALP, OPN, DSPP, OCN, DMP1, and RUNX2 were increased during the

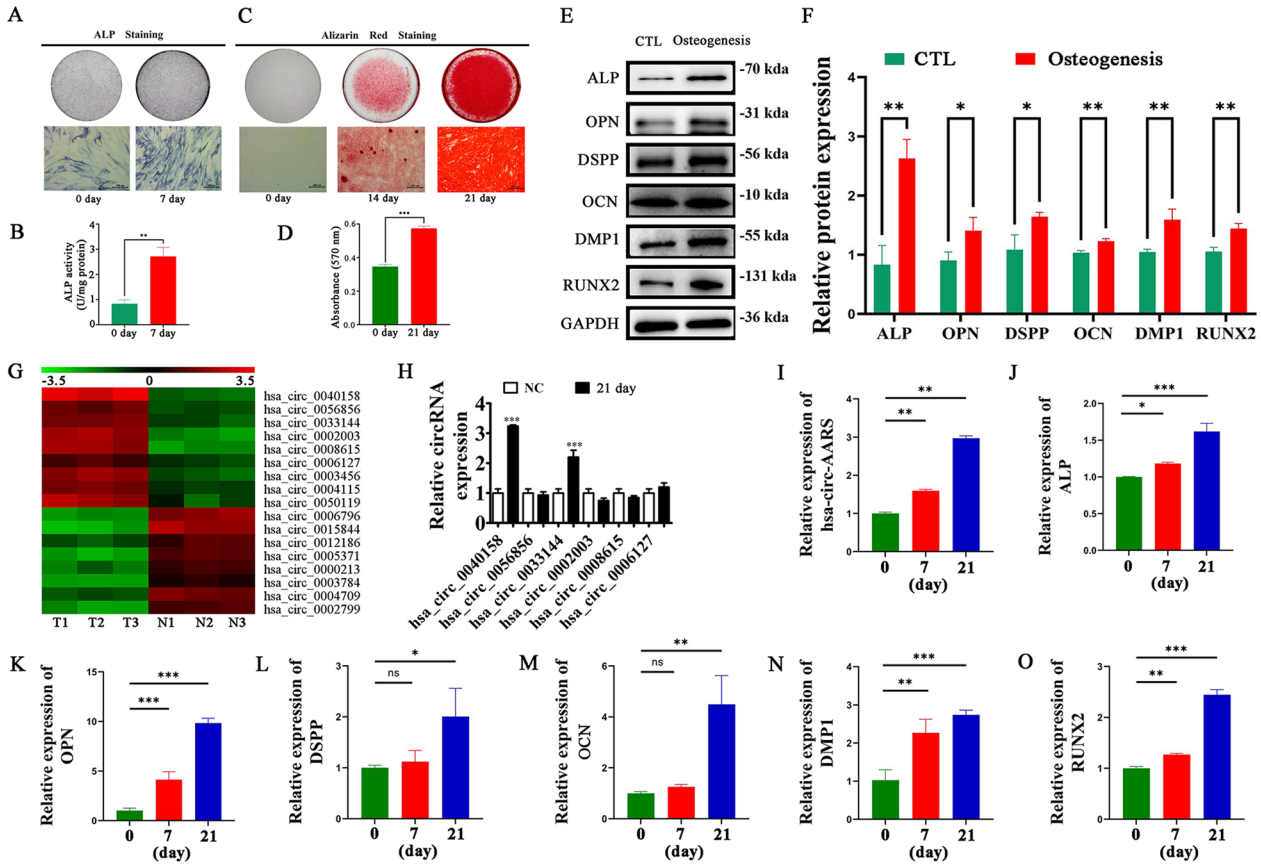

Fig. 2 circ-AARS plays a role during the odontogenic differentiation of DPSCs. **A** and **B** ALP staining showing the odontogenic differentiation of DPSCs. Data are expressed as mean ± SD. $^{**}p < 0.01$ versus 0 day. **C** and **D** ARS staining showing the odontogenic differentiation of DPSCs (scale bar = 200 μm). Data are expressed as mean ± SD. $^{***}p < 0.001$ versus 0 day. **E** and **F** Western blotting assay showing the relative expression levels of proteins involved in osteogenic differentiation. Data are expressed as mean ± SD. $^{*}p < 0.05$, $^{**}p < 0.01$ versus CTL. **G** Heatmap showing the differentially expressed circRNAs in DPSCs during odontogenic differentiation. T means odontogenic differentiation group. N means Normal group. **H** qRT-PCR analysis of circRNA expression in DPSCs during odontogenic differentiation. Data are expressed as mean ± SD. $^{***}p < 0.001$ versus NC. **I**–**O** qRT-PCR analysis showing the relative expression levels of genes associated with osteogenic differentiation in DPSCs. Data are expressed as mean ± SD. $^{*}p < 0.05$, $^{**}p < 0.01$, $^{***}p < 0.001$

odontogenic differentiation of DPSCs after circ-AARS upregulation (Fig. 5F–K). WB assay results confirmed that the protein expression levels of ALP, OPN, DSPP, OCN, DMP1, and RUNX2 were increased during the odontogenic differentiation of DPSCs after circ-AARS upregulation (Fig. 5L and M). These findings suggest that circ-AARS upregulation promotes the odontogenic differentiation of DPSCs.

Circ-AARS promotes the odontogenic differentiation of DPSCs by regulating miR-24-3p

Bioinformatics analysis (circBank and starBase database search and miRNA sequencing) confirmed that miR-24-3p was the downstream target of circ-AARS (Figure S1A). The dual-luciferase reporter analysis confirmed that miR-24-3p inhibited luciferase activity in wild-type cells, but not in mutated cells (Figure S1B and C), thus suggesting that miR-24-3p is the target of circ-AARS. qRT-PCR analysis showed that circ-AARS downregulation inhibited circ-AARS expression but promoted miR-24-3p expression. However, the inhibition of miR-24-3p expression did not restore circ-AARS expression. This finding suggests that miR-24-3p is the downstream target of circ-AARS. miR-24-3p downregulation inhibited the expression of miR-24-3p (Figure S1D and E). qRT-PCR analysis showed that miR-24-3p inhibition restored the relative expression levels of ALP, OPN, DSPP, OCN, DMP1, and RUNX2, all of which were involved in odontogenic differentiation after circ-AARS silencing (Figure S1F–K). Likewise, WB assay results also revealed that miR-24-3p inhibition restored the relative protein expression levels of ALP, OPN, OCN, DMP1, and RUNX2 (Figure S1L). This finding indicates that circ-AARS promotes

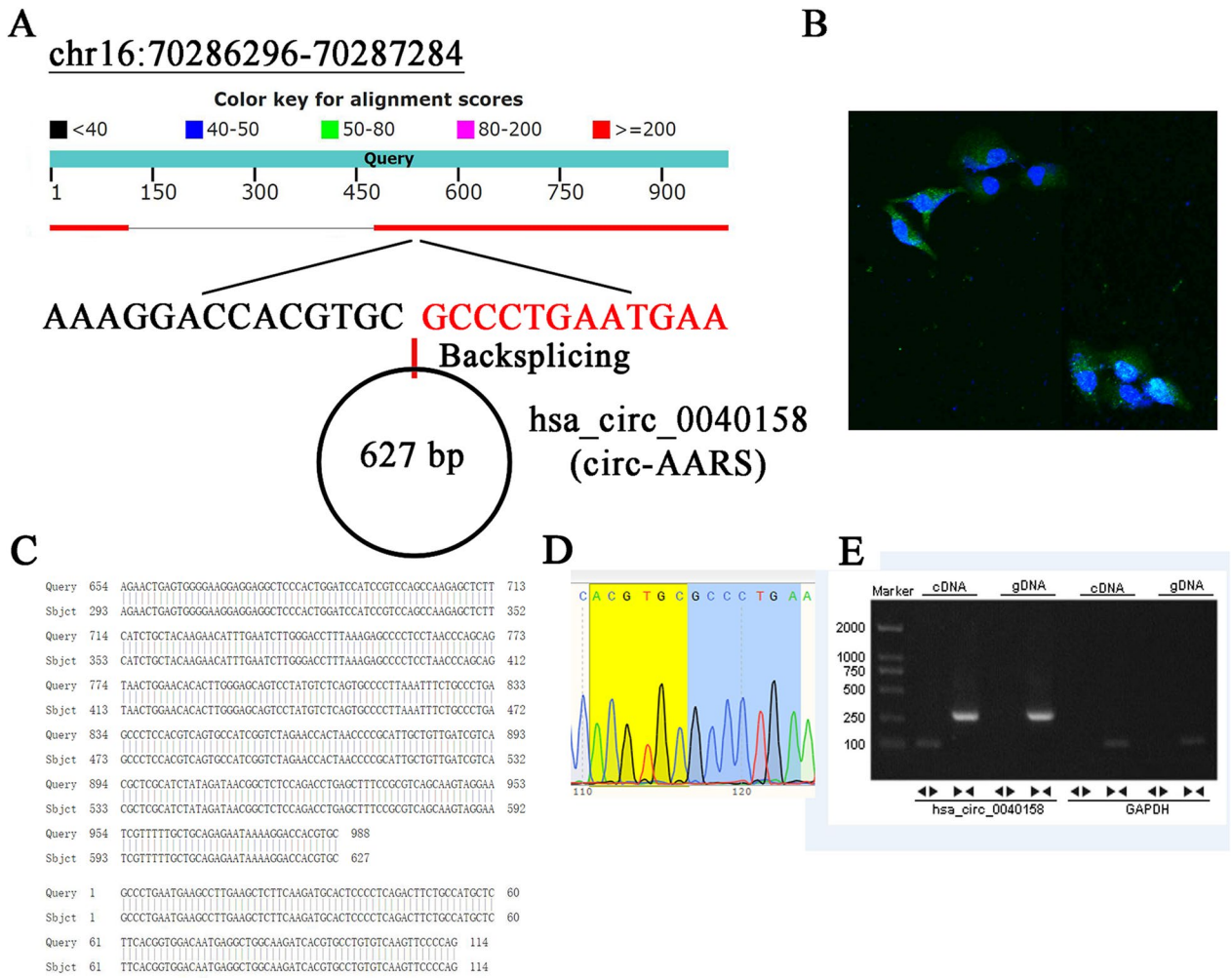

Fig. 3 The sequence of hsa_circ_0040158 and its expression in DPSCs. **A** Genomic loci of the AARS gene and hsa_circ_0040158. The red sign indicates the back-splicing junction. **B** The sequence of hsa_circ_0040158 and its expression in DPSCs as determined by fluorescence in situ hybridization (FISH) staining. **C** The sequence of hsa_circ_0040158. **D** Sanger sequencing assay confirmed the sequences amplified by divergent primers. **E** The amplification products obtained through divergent primers and convergent primers were separated by agarose gel electrophoresis

the odontogenic differentiation of DPSCs by regulating miR-24-3p.

Circ-AARS promotes the odontogenic differentiation of DPSCs by regulating KLF6

Based on the results of bioinformatics analysis (miRBD, TargetScan, and starBase database search and mRNA sequencing), KLF6 was confirmed to be the downstream target of miR-24-3p (Figure S2A). The dual-luciferase reporter assay demonstrated that miR-24-3p inhibited luciferase activity in wild-type cells, but not in mutated cells (Figure S2B and C), suggesting that the KLF6 3′-UTR- is the target of miR-24-3p. ALP staining (Figure S2D and E) and ARS staining (Figure S2F) showed that KLF6 overexpression restored the odontogenic differentiation ability of DPSCs after circ-AARS silencing. qRT-PCR analysis revealed that circ-AARS downregulation inhibited the expression of both circ-AARS and KLF6. However, KLF6 overexpression did not restore circ-AARS expression. This finding suggests that KLF6 is the downstream target of circ-AARS. KLF6 upregulation promoted KLF6 expression (Figure S2G and H). qRT-PCR analysis demonstrated that KLF6 overexpression restored the relative expression levels of the odontogenic differentiation genes ALP, OPN, DSPP, OCN, DMP1, and RUNX2 after circ-AARS silencing (Figure S2I–O). Additionally, WB assay results revealed that KLF6 overexpression restored the relative expression levels of the odontogenic differentiation proteins ALP, OPN, DSPP, OCN, DMP1, and RUNX2 after circ-AARS

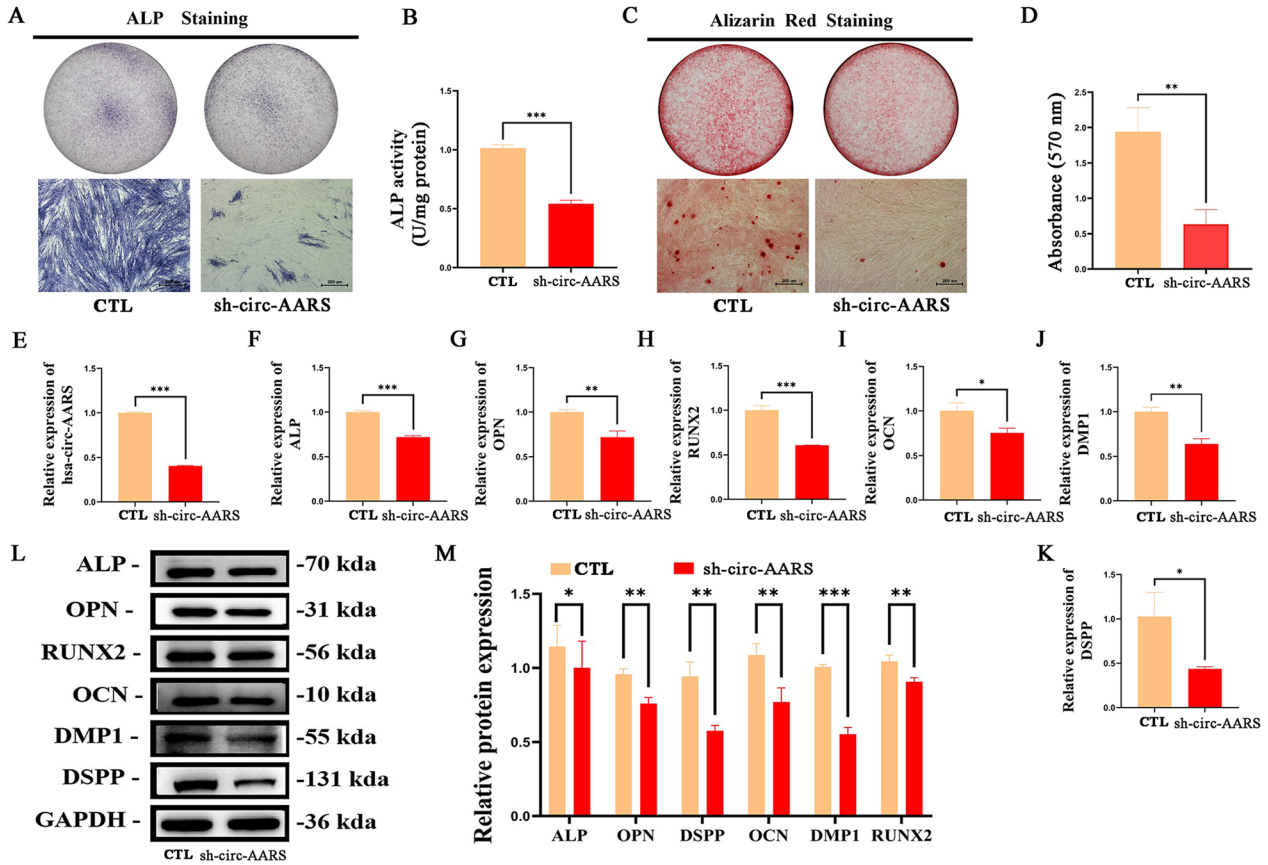

Fig. 4 circ-AARS downregulation inhibits the odontogenic differentiation of DPSCs. **A** and **B** ALP staining showing the odontogenic differentiation of DPSCs (scale bar = 200 μm). Data are expressed as mean ± SD. $^{***}p < 0.001$ versus CTL. **C** and **D** ARS staining showing the odontogenic differentiation of DPSCs (scale bar = 200 μm). Data are expressed as mean ± SD. $^{**}p < 0.01$ versus CTL. E–K qRT-PCR analysis showing the relative expression levels of genes associated with osteogenic differentiation. Data are expressed as mean ± SD. $^{*}p < 0.05$, $^{**}p < 0.01$, $^{***}p < 0.001$ vs. CTL. **L** and **M** Western blotting assay showing the relative expression levels of proteins involved in the osteogenic differentiation of DPSCs. Data are expressed as mean ± SD. $^{*}p < 0.05$, $^{**}p < 0.01$, $^{***}p < 0.001$

silencing (Figure S2P and Q). These findings suggest that circ-AARS promotes the odontogenic differentiation of DPSCs by regulating KLF6.

KLF6 overexpression reversed the inhibitory effect of miR-24-3p on the odontogenic differentiation of DPSCs

As observed in ALP staining (Figure S3A and B) and ARS staining (Figure S3C), miR-24-3p overexpression inhibited the odontogenic differentiation of DPSCs. However, KLF6 overexpression following miR-24-3p overexpression restored the odontogenic differentiation ability of DPSCs. qRT-PCR analysis showed that miR-24-3p upregulation promoted miR-24-3p expression and inhibited KLF6 expression. However, KLF6 overexpression did not restore miR-24-3p expression. This result suggests that KLF6 is the downstream target of miR-24-3p. KLF6 upregulation promoted the expression of KLF6 (Figure S2G and H). qRT-PCR analysis showed that KLF6 overexpression restored the relative expression levels of the odontogenic differentiation genes ALP, OPN, DSPP, OCN, DMP1, and RUNX2 after miR-24-3p overexpression (Figure S3F–K). These findings suggest that KLF6 overexpression reverses the inhibitory effect of miR-24-3p on the odontogenic differentiation of DPSCs.

Validation of the impact of circ-AARS on DPSCs through in vivo experiments

To clarify whether circ-AARS expression influences bone formation in vivo, DPSCs expressing sh-circ-AARS, lv-circ-AARS, and NC were loaded on Bio-Oss collagen scaffolds and implanted in the subcutaneous tissue of nude mice (five mice per group). The study design is shown in Figure S4A. After 4 weeks, the implantation samples were harvested and analyzed. The amount of bone tissue as observed in H&E staining (Figure S4B) and collagen arrangement observed as blue color in Masson's trichrome staining (Figure S4C) were significantly higher in implants containing

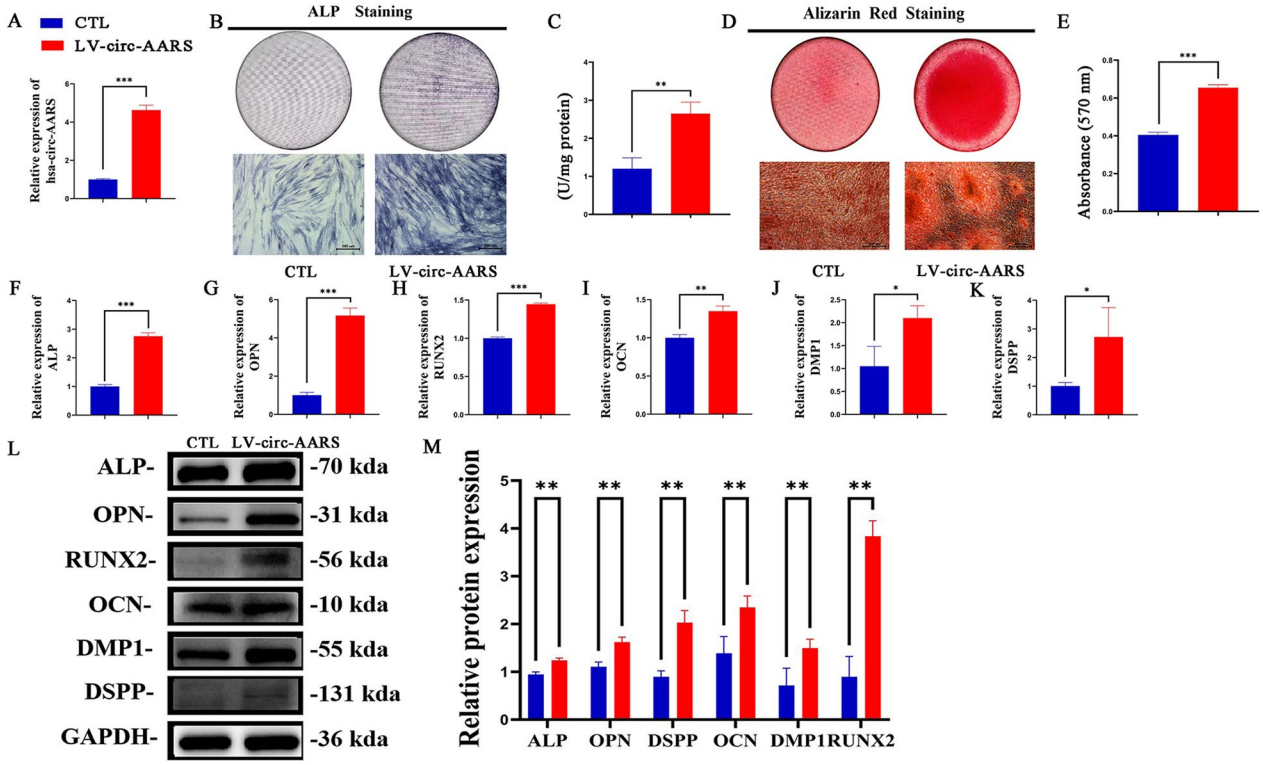

Fig. 5 circ-AARS upregulation promotes the odontogenic differentiation of DPSCs. **A** qRT-PCR analysis showing circ-AARS expression in DPSCs following transfection with the circ-AARS overexpression vector (LV-circ-AARS) or negative control (CTL). Data are expressed as mean ± SD. $^{***}p < 0.001$. **B** and **C** ALP staining showing the odontogenic differentiation of DPSCs (scale bar = 200 μm). Data are expressed as mean ± SD. $^{**}p < 0.01$ versus CTL. **D** and **E** ARS staining showing the odontogenic differentiation of DPSCs (scale bar = 200 μm). Data are expressed as mean ± SD. $^{***}p < 0.001$ versus CTL. **F**–**K** qRT-PCR analysis showing the relative expression levels of genes associated with osteogenic differentiation. Data are expressed as mean ± SD. $^{*}p < 0.05$, $^{**}p < 0.01$, $^{***}p < 0.001$ versus CTL. **L** and **M** Western blotting assay showing the relative expression levels of proteins involved in the osteogenic differentiation of DPSCs. Data are expressed as mean ± SD. $^{**}p < 0.01$

circ-AARS-overexpressing cells and lower in the sh-circ-AARS group. Osteoblasts and bone trabeculae were positive for BGLAP staining, as observed in IHC. The extent and intensity of staining were increased in the circ-AARS overexpression group and reduced in the circ-AARS downregulation group (Figure S4D).

Discussion

Stem cell therapies and tissue engineering have been proposed as useful strategies for treating damaged tissues and bone defects [10–12]. In the present study, we isolated DPSCs and found that DPSCs showed a typical shuttle-shaped morphology. We also noted that DPSCs have a odontogenic differentiation potential. Previous studies have confirmed that circRNA has an important role during odontogenic differentiation [13, 14]. To identify circRNAs with a differential expression pattern during odontogenic differentiation, DPSCs with or without odontogenic differentiation were subjected to high-throughput sequencing. The results showed that hsa_circ_0040158 expression was increased during the odontogenic differentiation of DPSCs. hsa_circ_0040158 originates from the exon of the AARS gene located at chr16:70,286,296–70287284. The AARS gene is 899 bp in length, and the spliced mature circRNA is 627 bp in length; therefore, we named hsa_circ_0040158 as circ-AARS. In the present study, we found that circ-AARS downregulation inhibited the odontogenic differentiation ability of DPSCs, while circ-AARS upregulation promoted their odontogenic differentiation ability. This result suggests that circ-AARS has a critical function during the odontogenic differentiation of DPSCs.

Bioinformatics analysis showed that circ-AARS interacts with miR-24-3p, which was confirmed by the dual-luciferase reporter assay. As reported in previous studies, TRIB3 promotes the osteogenic differentiation of human adipose-derived stem cells mediated by the post-transcriptional regulation of miR-24-3p [15]. miR-24-3p downregulation promotes the osteogenic differentiation of human periodontal ligament stem cells by targeting SMAD family member 5 [16]. The lncRNA LEF1-AS1 promotes the osteogenic differentiation of DPSCs by

sponging miR-24-3p [17]. In the present study we found that circ-AARS downregulation promotes miR-24-3p expression. Moreover, miR-24-3p inhibition restored the odontogenic differentiation ability of DPSCs after circ-AARS silencing. This finding indicates that circ-AARS promotes the odontogenic differentiation of DPSCs by regulating miR-24-3p.

Our further analysis revealed that KLF6 is also the downstream target of circ-AARS. KLF protein family members are known to activate and/or represses transcription in a promoter- and cell-dependent manner by interacting with co-suppressors or co-activators [18]. Recent evidence shows that KLF15 expression is increased in osteoblasts exposed, which can in turn regulate Wnt signaling transduction and bone formation [19]. Furthermore, miRNA-197-3p has been shown to inhibit osteogenic differentiation in osteoporosis by downregulating KLF10 expression [20]. Previous studies have also confirmed KLF6 expression levels were significantly elevated during odontogenic differentiation [21, 22]. In the present study, we found that circ-AARS downregulation inhibited KLF6 expression. However, KLF6 overexpression restored the odontogenic differentiation ability of DPSCs after circ-AARS silencing. This finding suggests that circ-AARS promotes the odontogenic differentiation of DPSCs by regulating KLF6.

As reported previously, circRNA regulates gene expression by sponging miRNAs [23, 24]. In the present study, the dual-luciferase reporter assay confirmed that miR-24-3p interacts with the KLF6 3′-UTR. miR-24-3p overexpression inhibited KLF6 expression and the odontogenic differentiation ability of DPSCs. However, KLF6 overexpression reversed the inhibitory effect of miR-24-3p on the odontogenic differentiation ability of DPSCs. Additionally, in vivo experiments in a heterotopic bone model confirmed that circ-AARS overexpression promotes the odontoblastic differentiation of DPSCs. Thus, these results suggest that circ-AARS promotes the odontoblastic differentiation of DPSCs by increasing KLF6 expression and sponging miR-24-3p.

Conclusion

Taken together, the present study shows that circ-AARS plays a crucial role during the odontogenic differentiation of DPSCs by modulating miR-24-3p/KLF6 expression (Figure S5). Our findings provide new insights regarding how circ-AARS influences the pulpitis process and reveal a potential therapeutic target for patients with dental defects.

Abbreviations

circRNAs	Circular RNAs
DPSCs	Dental pulp stem cells
ALP	Alkaline phosphatase
OD	Optical density
ARS	Alizarin red S
H&E	Hematoxylin-eosin
IHC	Immunohistochemistry

Supplementary Information

The online version contains supplementary material available at https://doi.org/10.1186/s13287-025-04239-z.

Additional file 1. Figure S1 circ-AARS promotes the odontogenic differentiation of DPSCs by regulating miR-24-3p. (A) Bioinformatics analysis showing miRNAs that interact with circ-AARS. (B) Bioinformatics analysis for predicting binding sites of miR-24-3p in circ-AARS. Mutant version of circ-AARS is shown. (C) Relative luciferase activity determined at 48 h after transfection of DPSCs with miR-24-3p mimic/NC or circ-AARS wild-type/Mut. Data are expressed as mean ± SD. ***p < 0.001. (D and E) qRT-PCR analysis showing the expression pattern of circ-AARS and miR-24-3p. Data are expressed as mean ± SD. ***p < 0.001. (F–L) qRT-PCR and western blotting assay showing the relative expression level of genes and proteins, respectively, associated with osteogenic differentiation. Data are expressed as mean ± SD. *p < 0.05, ***p < 0.001. Figure S2 circ-AARS promotes the odontogenic differentiation of DPSCs by regulating KLF6. (A) Bioinformatics analysis showing mRNAs that interact with miR-24-3p. (B) Bioinformatics analysis for predicting binding sites of miR-24-3p in KLF6. Mutant version of the KLF6 3′-UTR is shown. (C) Relative luciferase activity determined at 48 h after transfection of DPSCs with the miR-24-3p mimic/NC or KLF6 3′-UTR- wild-type/Mut. Data are expressed as mean ± SD. ***p < 0.001. (D–F) ALP staining and ARS staining showing the odontogenic differentiation of DPSCs (scale bar = 200 μm). Data are expressed as mean ± SD. *p < 0.05. (G and H) qRT-PCR analysis showing circ-AARS and KLF6 expression. Data are expressed as mean ± SD. ***p < 0.001. (I-O) qRT-PCR analysis showing the relative expression levels of genes associated with osteogenic differentiation. Data are expressed as mean ± SD. *p < 0.05, ***p < 0.001. (P–Q) Western blotting assay showing the relative expression levels of proteins involved in osteogenic differentiation. Data are expressed as mean ± SD. *p < 0.05, **p < 0.01. Figure S3 KLF6 overexpression reversed the inhibitory effect of miR-24-3p on the odontogenic differentiation of DPSCs. (A–C) ALP staining and ARS staining showing the odontogenic differentiation of DPSCs (scale bar = 200 μm). Data are expressed as mean ± SD. ***p < 0.001. (D and E) qRT-PCR analysis showing miR-24-3p and KLF6 expression. Data are expressed as mean ± SD. ***p < 0.001. (F-K) qRT-PCR analysis showing the relative expression levels of genes associated with osteogenic differentiation. Data are expressed as mean ± SD. *p < 0.05, ***p < 0.001. Figure S4. In vivo experiments for validating the impact of circ-AARS on DPSCs. (A) The process of transplanting DPSCs into nude mice. (B) Histological examination of tissue sections with hematoxylin and eosin staining. (C) Histological examination of tissue sections with Masson's trichrome staining. (D) Histological examination of tissue sections with immunohistochemical staining for BGLAP (scale bar = 200 μm). Figure S5 Graphical Abstract Figure. A graphical summary of the study is shown.

Funding

This work was supported by the National Natural Science Foundation of China (Grant No. 82170922).

Author details

[1]Department of General Dentistry, Shanghai Ninth People's Hospital, Shanghai Jiao Tong University School of Medicine, College of Stomatology, Shanghai Jiao Tong University, National Center for Stomatology, National Clinical Research Center for Oral Diseases, Shanghai Key Laboratory of Stomatology, Shanghai Research Institute of Stomatology, Shanghai Ninth People's Hospital, Shanghai Jiaotong University School of Medicine, Shanghai 200011, China. [2]Shanghai Key Laboratory of Molecular Imaging, Shanghai University of Medicine and Health Sciences, Shanghai 200092, China. [3]Department

of Stomatology, Kashi Prefecture Second People's Hospital, No 1, Jiankang Road, Kashi 844000, Xinjiang, China.

Received: 12 August 2024 Accepted: 17 February 2025
Published online: 13 March 2025

References

1. Xuan K, Li B, Guo H, Sun W, Kou X, He X, Zhang Y, Sun J, Liu A, Liao L, Liu S, Liu W, Chenghu H, Shi S, Jin Y. Deciduous autologous tooth stem cells regenerate dental pulp after implantation into injured teeth. Sci Transl Med. 2018. https://doi.org/10.1126/scitranslmed.aaf3227.
2. Boroviak T, Loos R, Lombard P, Okahara J, Behr R, Sasaki E, Nichols J, Smith A, Bertone P. Lineage-specific profiling delineates the emergence and progression of naive pluripotency in mammalian embryogenesis. Dev Cell. 2015;35:366–82.
3. Huang CC, Narayanan R, Alapati S, Ravindran S. Exosomes as biomimetic tools for stem cell differentiation: applications in dental pulp tissue regeneration. Biomaterials. 2016;111:103–15.
4. Barrett SP, Wang PL, Salzman J. Circular RNA biogenesis can proceed through an exon-containing lariat precursor. Elife. 2015;4:e07540.
5. Chen LL, Yang L. Regulation of circRNA biogenesis. RNA Biol. 2015;12:381–8.
6. Ji F, Pan J, Shen Z, Yang Z, Wang J, Bai X, Tao J. The circular RNA circRNA124534 promotes osteogenic differentiation of human dental pulp stem cells through modulation of the miR-496/β-Catenin pathway. Front Cell Dev Biol. 2020;8:230.
7. Liu Z, Liu Q, Chen S, Su H, Jiang T. Circular RNA Circ_0005564 promotes osteogenic differentiation of bone marrow mesenchymal cells in osteoporosis. Bioengineered. 2021;12:4911–23.
8. Ji F, Zhu L, Pan J, Shen Z, Yang Z, Wang J, Bai X, Lin Y, Tao J. hsa_circ_0026827 promotes osteoblast differentiation of human dental pulp stem cells through the beclin1 and RUNX1 signaling pathways by sponging miR-188-3p. Front Cell Dev Biol. 2020;8:470.
9. Nagendrababu V, Kishen A, Murray PE, Nekoofar MH, de Figueiredo JAP, Priya E, Jayaraman J, Pulikkotil SJ, Camilleri J, Silva RM, Dummer PMH. PRIASE 2021 guidelines for reporting animal studies in Endodontology: a consensus-based development. Int Endod J. 2021;54:848–57.
10. Graziano A, d'Aquino R, Laino G, Papaccio G. Dental pulp stem cells: a promising tool for bone regeneration. Stem Cell Rev. 2008;4:21–6.
11. Ballini A, Cantore S, Farronato D, Cirulli N, Inchingolo F, Papa F, Malcangi G, Inchingolo AD, Dipalma G, Sardaro N, Lippolis R, Santacroce L, Coscia MF, Pettini F, De Vito D, Scacco S. Periodontal disease and bone pathogenesis: the crosstalk between cytokines and porphyromonas gingivalis. J Biol Regul Homeost Agents. 2015;29:273–81.
12. Papaccio G, Graziano A, d'Aquino R, Graziano MF, Pirozzi G, Menditti D, De Rosa A, Carinci F, Laino G. Long-term cryopreservation of dental pulp stem cells (SBP-DPSCs) and their differentiated osteoblasts: a cell source for tissue repair. J Cell Physiol. 2006;208:319–25.
13. Zhang Y, Zhang H, Yuan G, Yang G. circKLF4 upregulates Klf4 and endoglin to promote odontoblastic differentiation of mouse dental papilla cells via sponging miRNA-1895 and miRNA-5046. Front Physiol. 2021;12:760223.
14. Li C, Jiang H. Altered expression of circular RNA in human dental pulp cells during odontogenic differentiation. Mol Med Rep. 2019;20:871–8.
15. Bai XS, Zhang P, Liu YS, Liu H, Lv LW, Zhou YS. TRIB3 promotes osteogenic differentiation of human adipose-derived mesenchymal stem cells levelled by post-transcriptional regulation of miR-24-3p. Chin J Dent Res. 2021;24:235–49.
16. Li Z, Sun Y, Cao S, Zhang J, Wei J. Downregulation of miR-24-3p promotes osteogenic differentiation of human periodontal ligament stem cells by targeting SMAD family member 5. J Cell Physiol. 2019;234:7411–9.
17. Wu Y, Lian K, Sun C. LncRNA LEF1-AS1 promotes osteogenic differentiation of dental pulp stem cells via sponging miR-24-3p. Mol Cell Biochem. 2020;475:161–9.
18. Weng J, Wu J, Chen W, Fan H, Liu H. KLF14 inhibits osteogenic differentiation of human bone marrow mesenchymal stem cells by downregulating WNT3A. Am J Transl Res. 2020;12:4445–55.
19. Yang Y, Su Y, Wang D, Chen Y, Liu Y, Luo S, Wu T, Cui L. Tanshinol rescues the impaired bone formation elicited by glucocorticoid involved in KLF15 pathway. Oxid Med Cell Longev. 2016;2016:1092746.
20. You M, Zhang L, Zhang X, Fu Y, Dong X. MicroRNA-197-3p inhibits the osteogenic differentiation in osteoporosis by down-regulating KLF 10. Clin Interv Aging. 2021;16:107–17.
21. Chen Z, Xie H, Yuan J, Lan Y, Xie Z. Kruppel-like factor 6 promotes odontoblastic differentiation through regulating the expression of dentine sialophosphoprotein and dentine matrix protein 1 genes. Int Endod J. 2021;54:572–84.
22. Chen Z, Wu W, Zheng C, Lan Y, Xie H, Xie Z. KLF6 facilitates differentiation of odontoblasts through modulating the expression of P21 in vitro. Int J Oral Sci. 2022;14:20.
23. Lei Q, Liang Z, Lei Q, Liang F, Ma J, Wang Z, He S. Analysis of circRNAs profile in TNF-α treated DPSC. BMC Oral Health. 2022;22:269.
24. Liang C, Li W, Huang Q, Wen Q. CircFKBP5 suppresses apoptosis and inflammation and promotes osteogenic differentiation. Int Dent J. 2023;73:377–86.

Publisher's Note